http://dx.doi.org/10.4314/gjpas.v19i1.22

GLOBAL JOURNAL OF PURE AND APPLIED SCIENCES VOL. 19, 2013: 169-181
COPYRIGHT© BACHUDO SCIENCE CO. LTD PRINTED IN NIGERIA ISSN 1118-0579
www.globaljournalseries.com, Email: info@globaljournalseries.com

CLIMATOLOGY OF AIR MASS TRAJECTORIES AND AEROSOL OPTICAL THICKNESS OVER OUAGADOUGOU

B. KORGO, J. C. ROGER AND J. BATHIEBO

(Received 17 May 2013; Revision Accepted 22 November 2013)

ABSTRACT

We present in this paper a climatological study of back trajectories of air masses over Ouagadougou using the HYSPLIT model. The seasonal variability of the 300m, 1000m and 3000m wind trajectories were studied after a discussion related to the accuracy of trajectory models based on the work of Stohl. To this is added the climatology of the optical thickness at 675nm obtained by inversion of photometric measurements of AERONET network. A link was established between the backward trajectories and the aerosol optical thickness. An important conclusion of this approach has been to identify one of the main aerosol sources that influence the atmospheric optical properties over Ouagadougou especially during major dust events.

KEYWORDS: 1-backward trajectories, 2-aerosol optical thickness, 3- mineral dust, 4-HYSPLIT, 5-AERONET

INTRODUCTION

It is well known that the trajectories of air masses are useful in the study of weather phenomena, meteorology, dispersion of pollutants, in the process of lifting and transport of atmospheric aerosols and even in health. We can cite, for example, the identification of pathways of desert dust (Chiapello et *al*. , 1997) of water vapor transport (D'Abreton and tyson, 1996), the establishment of source-receptor relationship of air pollutant (Stohl, 1996), detection of sources of illegal production of drugs through the study of pollen transport (Cabezudo et *al*. , 1997). Ouagadougou is the capital of Burkina Faso, a landlocked country located in the heart of West Africa. Ouagadougou is located in the central region of the country. Geographically, its position is at latitude 12 ° North and longitude 1 °40 west. In terms of climate it is positioned in the semi -arid zone between the arid Sahel region adjacent in the north to the Sahara desert and dry sub-humid areas in the South. This gives the city a strategic position in the study of the trajectories of air masses in West Africa. Especially when we know that the Sahara is the largest desert with an area of 8.5 million km^2 (Laurent, 2005) and the largest source of dust in the world (Prospero et *al*., 2002). Annual emissions are estimated between 400 and 700 Mt (Schutz et *al*., 1987; D'Almeida, 1987; Swap *et al*., 1992; Laurent *et al*., 2008). Lifting and transport in the atmosphere of such a quantity of aerosols modify the optical properties of the atmosphere, and affect the radiative forcing. The objective of this paper is to perform a climatology of air masses backward trajectories at 300m, 1000m and 3000m over Ouagadougou and establish their connection with the variability of the aerosol optical thickness (AOT).

1 DATA AND METHODOLOGY

The data collected for this study are backward trajectories computed with the hybrid particle single integrated trajectory (HYSPLIT) model. It is more than 1500 trajectories from 2001 to 2010 at heights of 300m, 1000m and 3000m AGL. Theses heights are chosen because they allow the study of air motion in the atmospheric boundary layer is which is the seat of atmospheric turbulence that strongly influence the meteorology and dispersion (300m and 1000m) and also in the free troposphere where occurs the long-range transport of aerosols (3000m). The trajectories are computed for the entire period at intervals ranging from 2 to 3days and at different times of the day or night, because a first analysis of the HYSPLIT model trajectories computed has shown no significant daily variability. In addition, we used the photometric data of AERONET (Aerosol Robotic Network), to study the variability of the optical thickness. The AOT at 675 nm measured by Cimel sun / sky photometers were extracted from level 2 data (quality assured data) and coupled with the trajectories analyzed.

B. Korgo, Laboratoire des Energies Thermiques et Renouvelables (LETRE), Department de Physique, Université de Ouagadougou, Burkina Faso.
J. C. Roger, Laboratoire de Météorologie Physique (LaMP), Département de Physique, Université Blaise Pascal, Clermont-Ferrand, France.
J. Bathiebo, Laboratoire des Energies Thermiques et Renouvelables (LETRE), Department de Physique, Université de Ouagadougou, Burkina Faso.

1.1 THE HYSPLIT MODEL

There are two ways to simulate the movement of air masses in time and space: the Eulerian model and the Lagrangian model (Byers, 1974, Dutton, 1986). The Eulerian model considers fixed points of the space through which air masses circulate while the Lagrangian model is based on the spatio-temporal movement of an air parcel (Stohl, 1998).

The HYSPLIT trajectory, as its name suggests, is a hybrid between the Eulerian and Lagrangian approaches. The advection and diffusion are made in the Lagrangian framework, while the concentrations are calculated on a fixed grid (Draxler, 1998). The trajectory model provides a description of the position X of an air parcel at time t as a time-dependent function and its position X_0 at the time t_0 as follows:

$$X\ (t) = X\ (X_0,\ t) \tag{1}$$

All positions X (t) describes the forward trajectory of the point X_0. The coordinates of the position X_0 at the initial time t are called Lagrangian coordinates (Dutton, 1986). The inverse transform gives the expression of $X_0(t_0)$ as a function of X (t) and t as follows:

$$X_0\ (t_0) = X_0\ (X,\ t) \tag{2}$$

This transformation allows to describe the backward trajectory. The function X (X_0, t) is the solution path defined by the equation:

$$\frac{\mathrm{dX}}{\mathrm{dt}} = V(x,t) \tag{3}$$

where V (x, t) represents the speed of the wind vector at time t .The analytical solution of the trajectory equation can be obtained using the finite difference approximation of the development that gives X (t) as a Taylor series at the instant $t_1 = t_0+\Delta t$. We then obtain:

$$\mathrm{X}(t_1) = \mathrm{X}(t_0) + (\Delta t)\frac{\mathrm{dX}}{\mathrm{d}t}\bigg|_{t_0} + \frac{1}{2}(\Delta t)^2\frac{\mathrm{d}^2\mathrm{X}}{\mathrm{d}t^2}\bigg|_{t_0} + \cdots \tag{4}$$

The first approximation of this equation, simple solution of zero acceleration is of the form:

$$\mathrm{X}(t_1) \approx \mathrm{X}(t_0) + (\Delta t)\dot{\mathrm{X}}(t_0) \tag{5}$$

The development of X in Taylor's series at $t_0=t_1-\Delta t$ gives:

$$\mathrm{X}(t_0) = \mathrm{X}(t_1) - (\Delta t)\frac{\mathrm{dX}}{\mathrm{d}t}\bigg|_{t_1} + \frac{1}{2}(\Delta t)^2\frac{\mathrm{d}^2\mathrm{X}}{\mathrm{d}t^2}\bigg|_{t_1} - \cdots \tag{6}$$

The combination of two developments above gives the following expression for X (t_1):

$$\mathrm{X}(t_1) = \mathrm{X}(t_0) + \frac{1}{2}(\Delta t)[\dot{\mathrm{X}}(t_0) + \dot{\mathrm{X}}(t_1)] \quad + \frac{1}{4}(\Delta t)^2\left[\frac{\mathrm{d}\dot{\mathrm{X}}}{\mathrm{d}t}\bigg|_{t_0} - \frac{\mathrm{d}\dot{\mathrm{X}}}{\mathrm{d}t}\bigg|_{t_1}\right] + \cdots \tag{7}$$

The first approximation of the solution is:

$$\mathrm{X}(t_1) \approx \mathrm{X}(t_0) + \tfrac{1}{2}(\Delta t)[\dot{\mathrm{X}}(t_0) + \dot{\mathrm{X}}(t_1)] \tag{8}$$

This solution corresponds exactly to the one discribed by Draxler (1998) in the Hisplyt 4 modeling system for trajectories, dispersion and deposition, which is presented as follows:

$$P(t+\Delta t) = P(t)+0.5\ [\ V(P,t) + V(P',t+\Delta t)]\ \Delta t \tag{9}$$

In this expression, P(t) is the three-dimensional position at the reference instant t, P(t+Δt) at the time t + Δt , V (P, T) and V (P ' , t + At) the position vectors of the wind at times t and t+Δt respectively.
The errors associated with trajectory modeling have been widely studied by Stohl (1998), they are of five types:

- The truncation errors related to approximation by the method of finite difference which neglect the terms of high order of theTaylors' series (Walmsley and Mailhot, 1983, Seibert 1997).

- The interpolation errors due to interpolations between gridded wind fields which are based on the trajectory models and the radiosonde measurements (Karl and Samson, 1986, 1988a, 1988b; Stohl *et al.*, 1995; Draxler, 1996).

- Errors resulting and from asumptions Regarding the vertical wind, because unlike the horizontal wind, vertical component of the wind is obtained from meteorological models that are less accurate than the measurement results (Sardeshmuhk and Liebmann, 1993; Martin et *al* , 1987; Draxler , 1996a; Stohl and Seibert, 1997).

- Wind field errors, are in most of the cases either forecast errors or analysis errors. A lot of studies using different techniques by Maryon and Heasman (1988), Stunder (1996); Kahl *et al*. (1989a), and Pickering *et al*. (1994) Have Shown forecast errors ranging from 16 to 60 % depending on the travel time, the kind of trajectory (isentropic, isobaric, three-dimensional.)

- Starting position errors. The starting position is often not known with precision. A small error in the initial position can cause large errors amplification convergence or divergence of the flow (Baumann and Stohl (1993), kahl (1996), Merrill *et al.* (1985)).

Despite these sources of errors, the trajectory models that have known several improvements for decades have been successfully used in the study of transport, dispersion and deposition of particles and air pollutants (Tyson *et al.* 1996) and as specified by Draxler, the HYSPLIT model is designed for quick response to atmospheric emergencies, diagnostic case studies and climatological analyzes.

1.2 THE AERONET INVERSION

The AERONET network is made of CIMEL sun / sky radiometers installed worldwide. These radiometers measure the direct and diffuse radiation from which AERONET inversion code provides aerosol optical properties, radiative properties and microphysical properties in the total atmospheric column for different wavelengths. The optical properties inversed are the aerosol optical thickness (AOT), the Angstrom exponent, the real and imaginary part of the refractive index. The microphysical properties are the particle size distribution, the rate of sphericity and the radiative properties are shown by the single scattering albedo, the phase function, the asymmetry parameter, the spectral fluxes, the radiative forcing and the radiative forcing efficiency. The development of AERONET inversion codes are described in papers by Dubovik and King, (2000), Dubovik *et al.* (2000) Dubovik *et al.* (2002a), Dubovik *et al.*,(2002b), Dubovik *et al*., (2006a), Sinyuk *et al*., (2006)

The aerosol optical thickness (AOT) is a dimensionless number that characterizes the transparency of the atmosphere through the sunlight. It is defined by the fraction of electromagnetic radiation or light scattered or absorbed by the components of the atmosphere at a given wavelength. If I_0 is the intensity of the radiation emitted by the sun and I the intensity of the radiation which reaches the surface of the earth , τ the optical thickness of the atmospheric layer crossed is obtained by the following relationship:

$$\frac{I}{I_0} = e^{-\tau} \quad \text{or} \quad \tau = -\ln(\frac{I}{I_0}) \qquad (10)$$

For a transparent atmosphere, where there is almost no loss of energy, the optical thickness is close to zero. High optical thickness indicates a relatively loaded aerosols and therefore not transparent atmosphere. A sharp drop in visibility is associated with high value of the optical thickness.

2 RESULTS

2.1 THE BACKWARD TRAJECTORIES

2.1.1 The 300m trajectories.

The climatological analysis of the trajectories computed with HYSPLIT model shows a well-marked seasonal variability showing the succession of the monsoon and harmattan cycles in West Africa.

• At 300m above sea level, the backward trajectories over Ouagadougou are from North and North -East from November to March. During this period, the winds generally come from the Mediterranean, describe curves through either southern Libya, northern Chad and crossing an important part of Niger, or by Algeria and northern Mali and eastern Niger. Some of these winds reach Ouagadougou by the Atlantic through the Mauritanian coast or southern Morocco and northern Mali (fig.1(a); fig.1(b); fig.1(c)).

• From May to October the trajectories are mostly towards the South, Southwest from the Gulf of Guinea. In most cases they go through the Ivorian coast and travel across the country from South to North and sometimes a part of Ghana. Some of these paths pass through the Liberian and Guinean coast (fig.1(e); fig.1(f)).

• The April knows the particularity of having trajectories that alternate between North East and South West; some being marked than the others from one year to another (fig.1(c); fig.1(d)). It corresponds to the transition between the two seasons described. Generally, the south trajectories dominate from the end of the second week. Also in November, and sometime in March, despite the preponderance of Northeast winds, frequent intrusions Southwest winds are observed (fig.1(g); fig.1(h)).

2.1.2 The 1000m trajectories

An overview of the 1000m trajectories shows a similar seasonal variability to those of 300m. However, they frequently diverge from the trajectories 300m. If globally from November to March they have the north and north- easterly direction, these trajectories often deviate southward, coming from the Guinean gulf and from southeast over part of Nigeria, Northern Benin and Northern Togo (fig.(j)).

From May to October, the general trend of the trajectories marked by the south and southwest direction. A significant part of these trajectories diverge to the east or west paths 300m, often reaching Ouagadougou from Guinea or from Nigeria (fig.(i)).

2.1.3 The 3000m trajectories

The 3000m trajectories do not follow the seasonal variability described above. They have strong directional changes that occur with large differences in direction from even opposite trajectories in the same period. Unlike paths 300 and 1000m, the direction North and Northeast is observed throughout the year although the occurrence of these winds varies from one month to another. This direction is dominant in the period between the months of March and November , which means that the trajectories are opposed in the majority of cases the air masses of 300 and 1000m that have at that time the South and southwest direction (fig.1(c); fig.1(d); fig.1(e); fig.1(f)).

In the period extending from December to February, the changes are more significant to the point where it is difficult to identify a dominant direction. In addition to the North and northeast paths, many east and southeast paths are observed, but also some from the South and West. Most of the variations of the trajectory directions are observed in the month of January (fig.1(a); fig.1(b)).

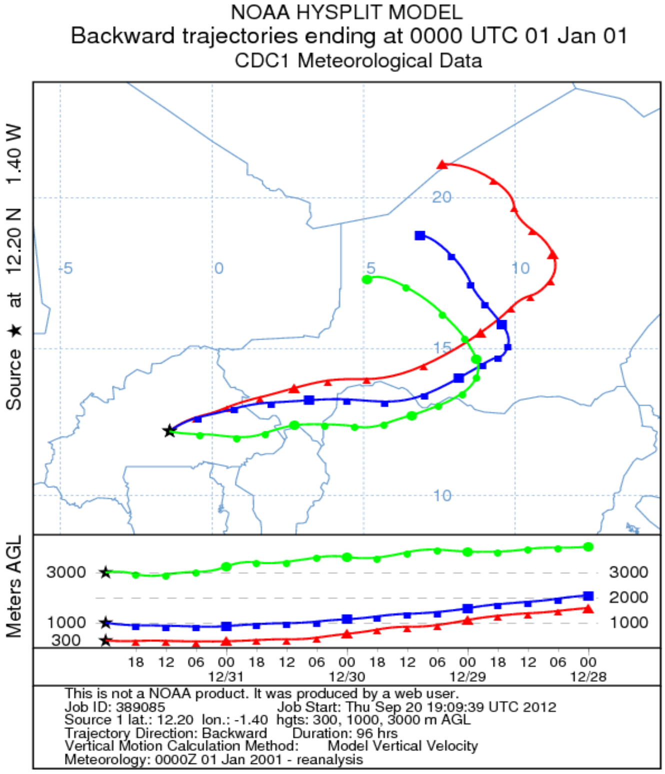

NOAA HYSPLIT MODEL
Backward trajectories ending at 0000 UTC 01 Jan 01
CDC1 Meteorological Data

This is not a NOAA product. It was produced by a web user.
Job ID: 389085 Job Start: Thu Sep 20 19:09:39 UTC 2012
Source 1 lat.: 12.20 lon.: -1.40 hgts: 300, 1000, 3000 m AGL
Trajectory Direction: Backward Duration: 96 hrs
Vertical Motion Calculation Method: Model Vertical Velocity
Meteorology: 0000Z 01 Jan 2001 - reanalysis

Fig.1(a)

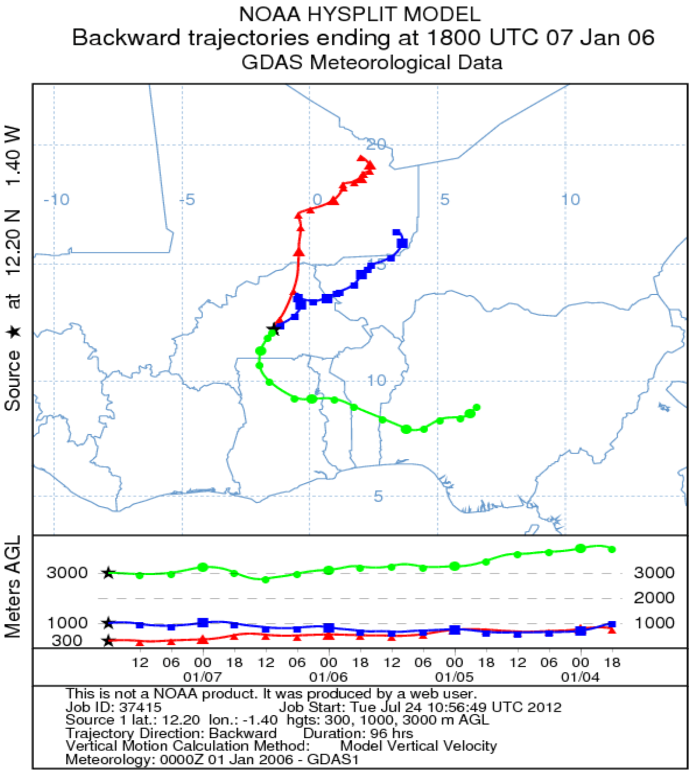

NOAA HYSPLIT MODEL
Backward trajectories ending at 1800 UTC 07 Jan 06
GDAS Meteorological Data

This is not a NOAA product. It was produced by a web user.
Job ID: 37415 Job Start: Tue Jul 24 10:56:49 UTC 2012
Source 1 lat.: 12.20 lon.: -1.40 hgts: 300, 1000, 3000 m AGL
Trajectory Direction: Backward Duration: 96 hrs
Vertical Motion Calculation Method: Model Vertical Velocity
Meteorology: 0000Z 01 Jan 2006 - GDAS1

fig.1(b)

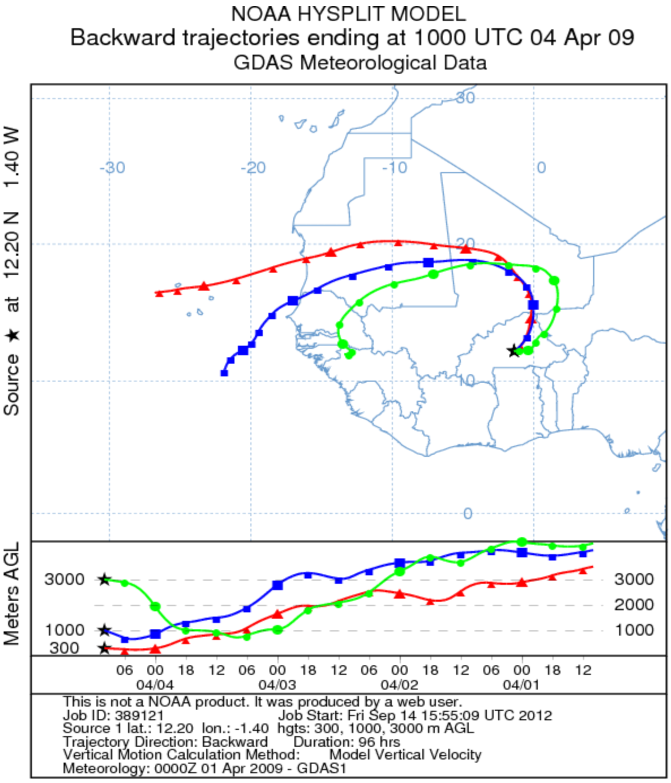

fig.1(c)

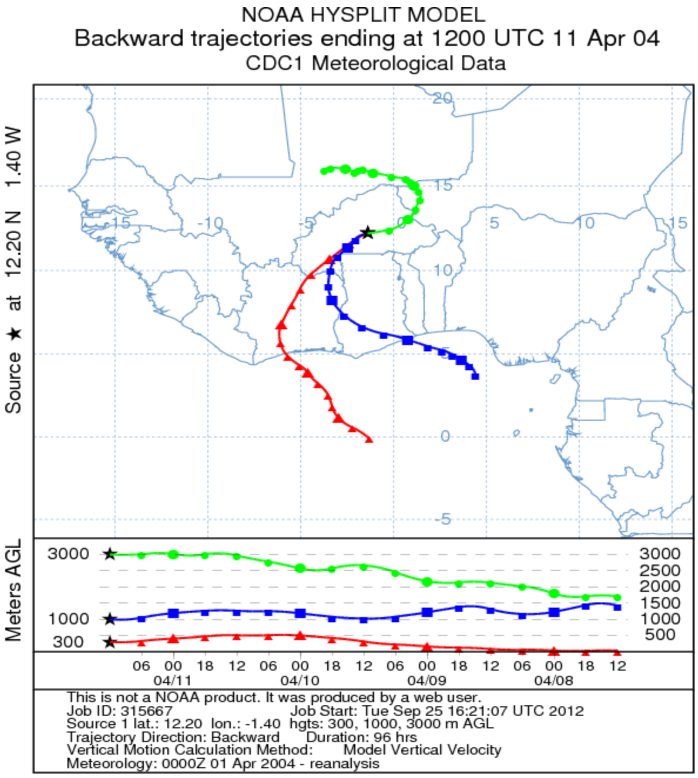

fig.1(d)

The Northeast and north direction of 300 and 1000m trajectories are seen in January while the 3000m trajectories present Northeast and south directions (fig 1(a) and fig.1(b)). In April the 300m and 1000m trajectories aternate between Noth and south direction(fig.1(c),fig.1(d))

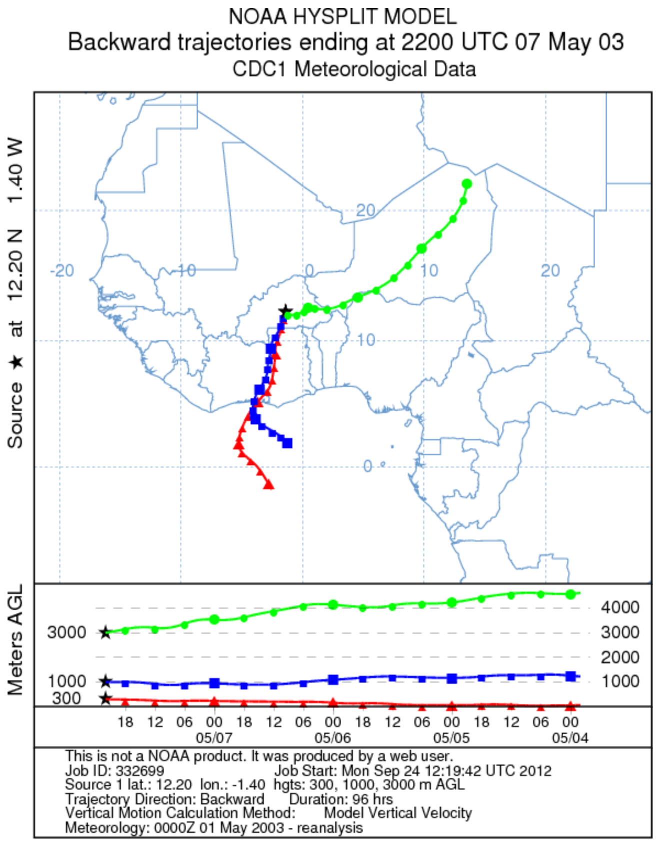

Fig.1 (e)

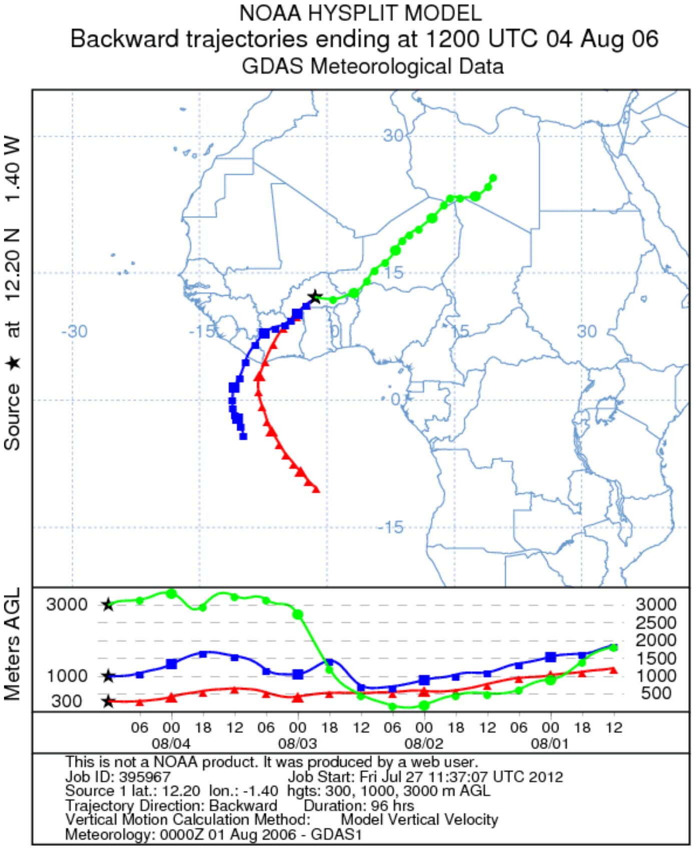

Fig.1 (f)

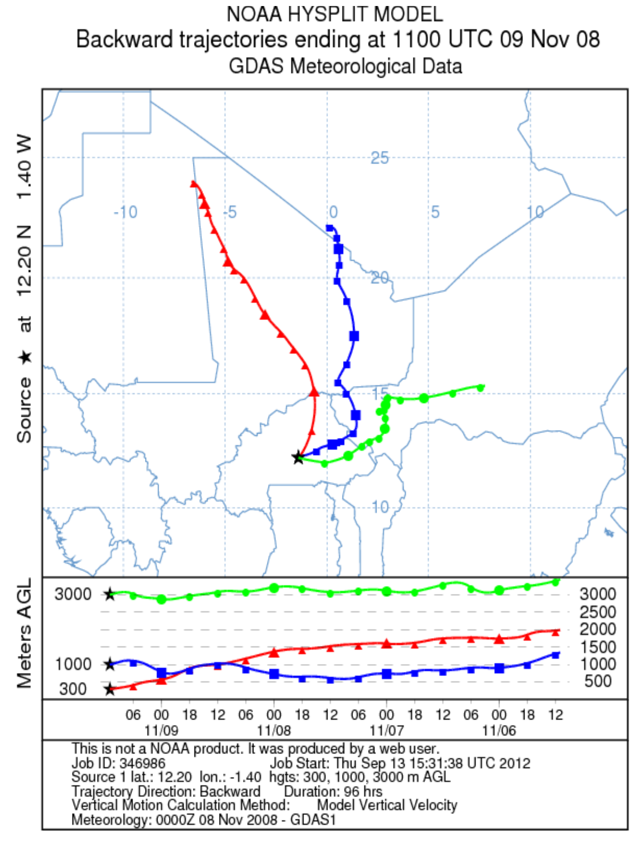

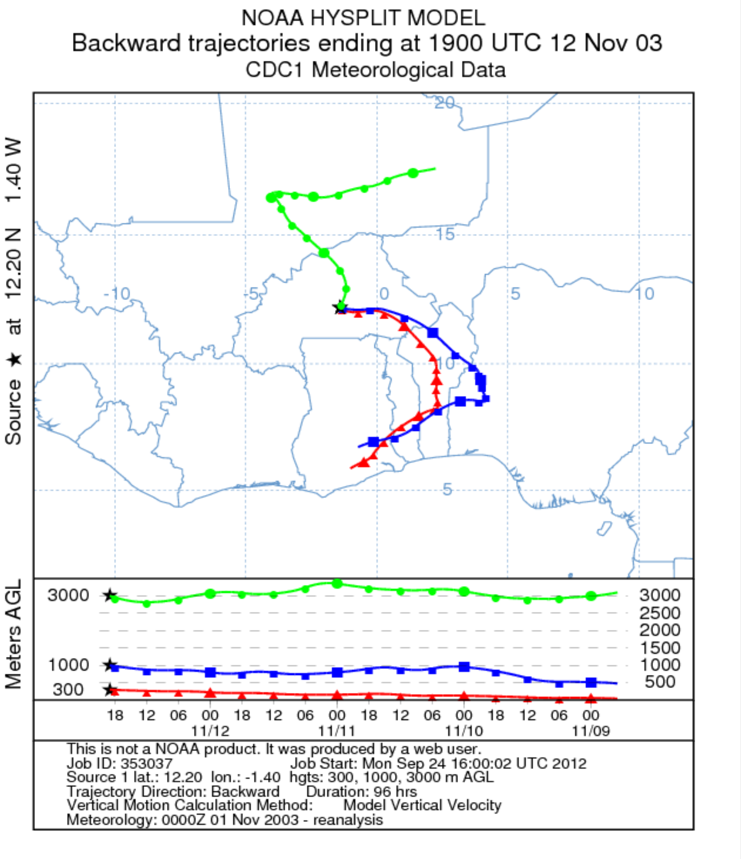

fig.1(g)

fig.1(h)

Southwest direction of 300m and 1000m winds, northern direction of 3000m winds during the rainy season from May to september(fig.1(e), fig.1(f)). On November the 300m and 1000m alternate south and north (fig.1(g), fig.1(h)).

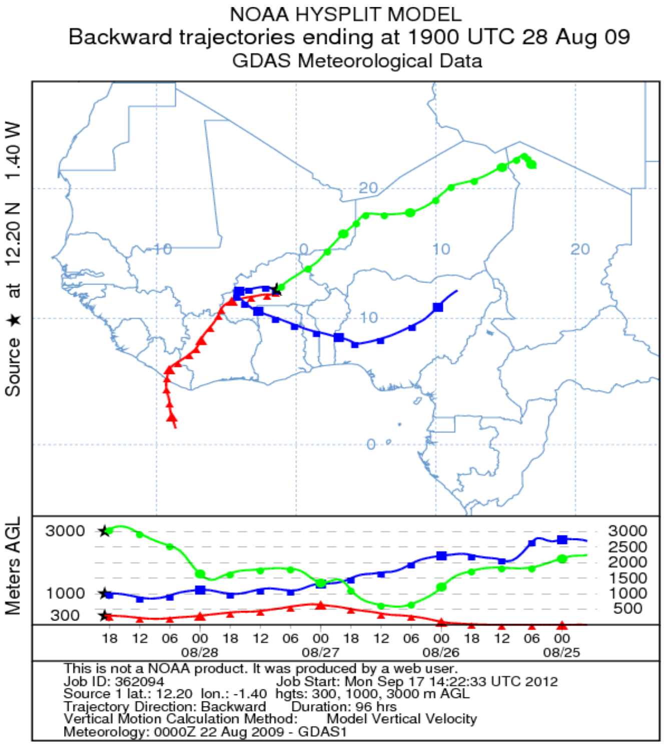

Fig.1(i)

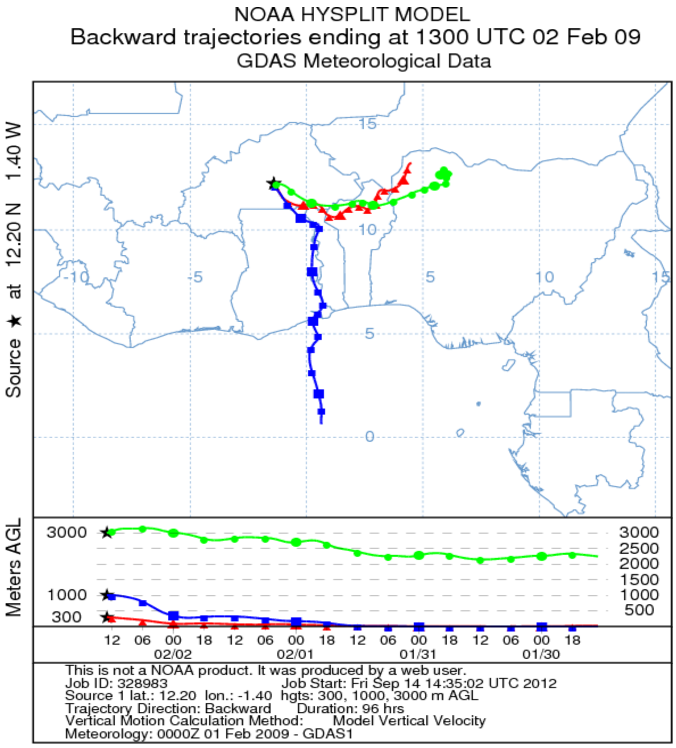

fig.1(j)

Deviation of the 1000m trajectories from that of 300m, coming from the southeast (fig.6(i)) and from the Guinean gulf in the south (fig.6(j))

2.2 THE AEROSOL OPTICAL THICKNESS

Based on the data measured on the AERONET site of Ouagadougou from 1998 to 2006, it is clear that the optical thickness is characterized by a well-marked seasonal variability. The high values are recorded in the period of predominance of harmattan winds, with annual peaks observed almost on a regularly between the months of February and March. These peaks can exceed values of 2.5 or 3 (fig.2). This is what shows the figure below using photometric measurements points at 675 nm. The low values of AOT are recorded during the monsoon season and highlight the hydrophobic nature of aerosols and suggest the dominance of desert aerosols that are difficult to mobilize in that period due to soil moisture or leached by rainfall.

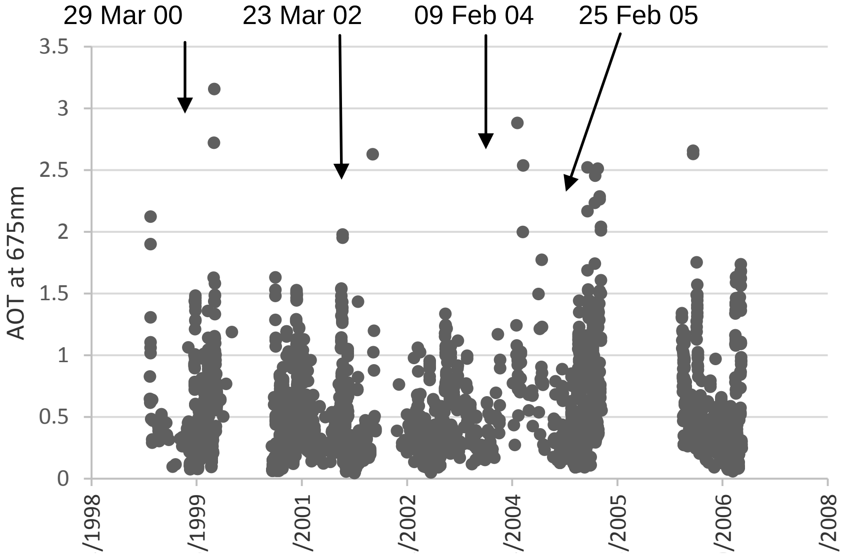

Fig.2: AOT, 675nm at Ouagadougou

Secondary peaks are recorded in the months of May and October. These periods correspond to transitions between wet and dry seasons. In May, the meeting between the monsoon winds and harmattan causes convection which involves dust particles. In October the end of the rainy season causes the drying of soils and sediments deposited by rainwater can be mobilized by the harmattan winds prevailing again in the north-east direction. This can be clearly seen with the monthly average of the optical thicknesses that show periodic variations with peaks in February / March.

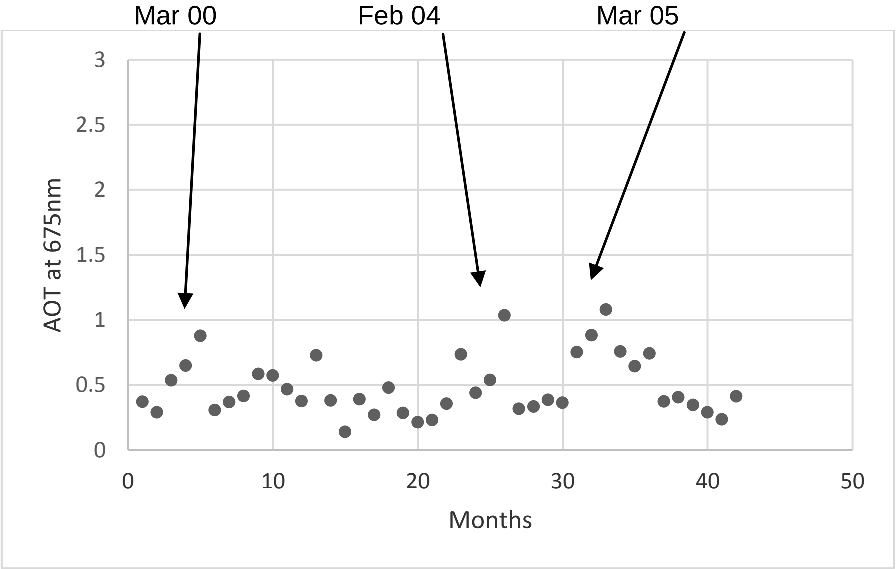

Fig.3: Monthly everage of AOT 675nm at Ouagadougou

The measurement site of AERONET network Ouagadougou worked intermittently from 1999 to 2006. This is the reason why, our observations were supplemented by measurements of the nearest site. This is Banizoumbou Niger, located at about 500km north-east of Ouagadougou, where measures have been more regular. The same type of variability was observed as shown in the following figure, obtained with of photometric measurements from 1995 to 2007:

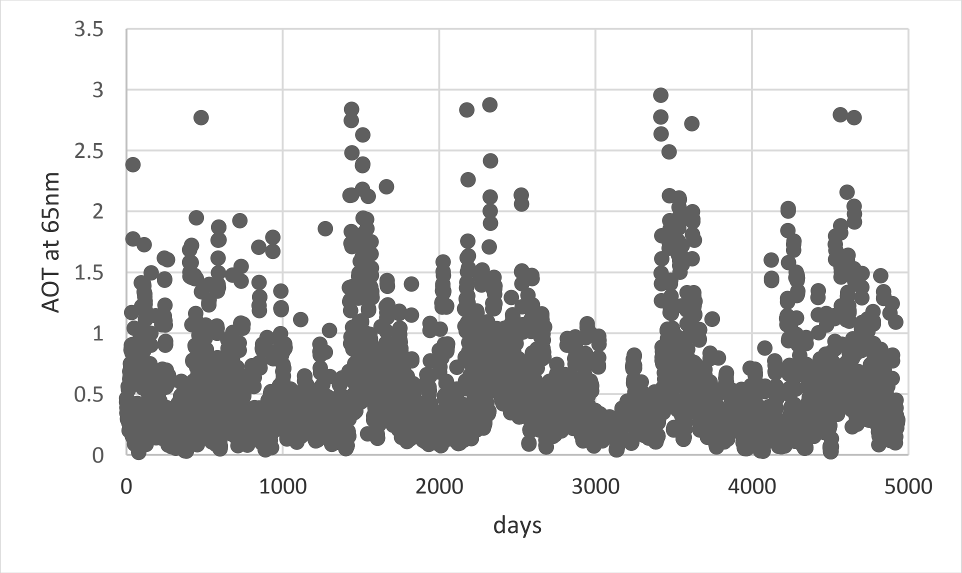

Fig.4: AOT, 675nm at Banizoumbou, Niger

The hydrophobic nature of aerosols can be clearly seen by coupling the optical thickness with water vapor (fig.5). We clearly see the decrease of the monthly average of the optical thickness with increasing water vapor between the months of June and October.

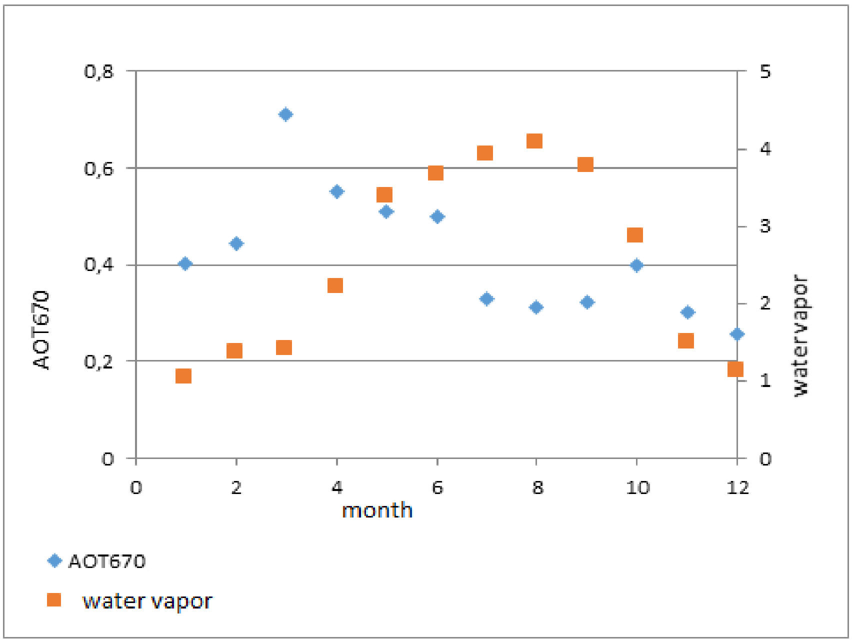

Fig.5: Monthly average of AOT and water vapor, Ouagadougou

Analysis of trajectories of days of optical thickness peaks shows the influence Saharan dust events of large scale extending over an important part of West Africa. The trajectories of lower tropospheric layers (300 and 1000m) are particularly marked by the consistency of the northern and north-eastern origin. These air masses cross through a large part of Niger (Niamey region) and Chad (fig.6(a), fig.6(d), fig.6(g)), where is located Bodélé depression zone characterized by an intense lifting and qualified as the first source of mineral aerosols in the world (Middleton and Goudie, 2001; Prospero *et al.*, 2002; Washington *et al*, 2003). This is clearly seen by looking at the optical thickness of Banizoumbou where peaks of aerosols between February and March are measured in one or two days before those of Ouagadougou. This shows the influence on Ouagadougou of the Bodele depression and the importance of low layer air masses in transport of dust to Ouagadougou, although it must not be overlooked the importance in this period of biomass burning and local uprisings. According to the data obtained, we can give examples of March 21, 2002 in Niamey against that of 23 March 2002 in Ouagadougou (fig6(b); fig.6(c)), February 7, 2004 in Niamey against that of February 9, 2004 in Ouagadougou (fig.6(e), fig.6(f)), February 11, 2005 in Niamey against that of February 12, 2005 in Ouagadougou and 25 February 2005 in Niamey and Ouagadougou (fig.6(h); fig.6(i)).

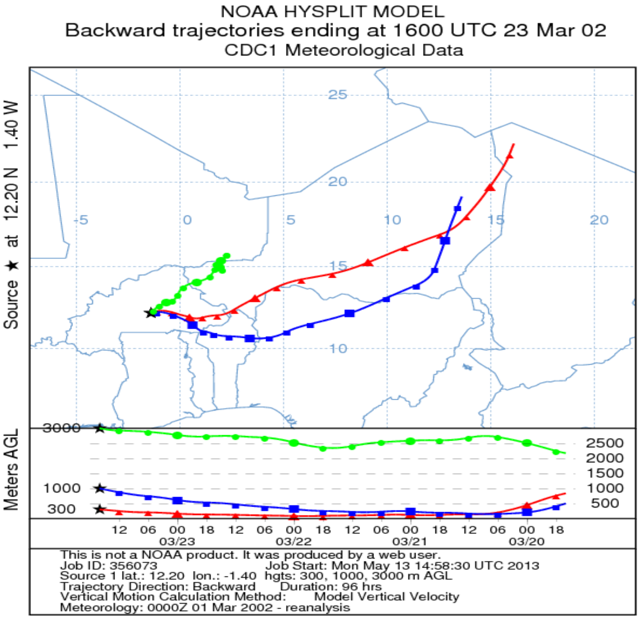

Fig.6(a): Backward trajectories Ouagadougou March 23, 2002

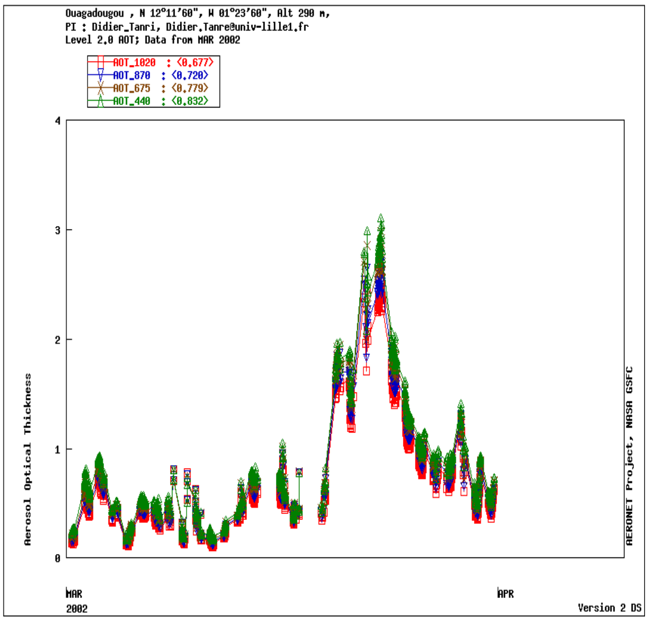

Fig.6(b): Ouagadougou AOT peak of March 23, 2002

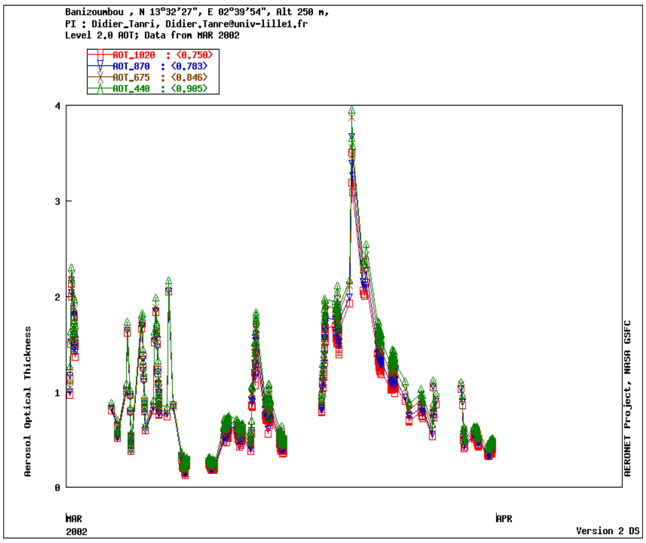

Fig.6(c): Banizoumbou AOT peak of March 21, 2002

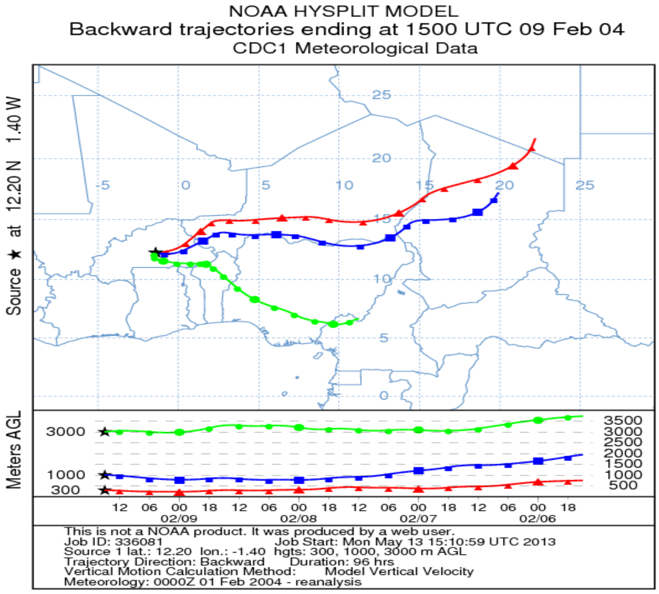

Fig.6(d): Backward trajectories, Ouagadougou Feb 09, 2004

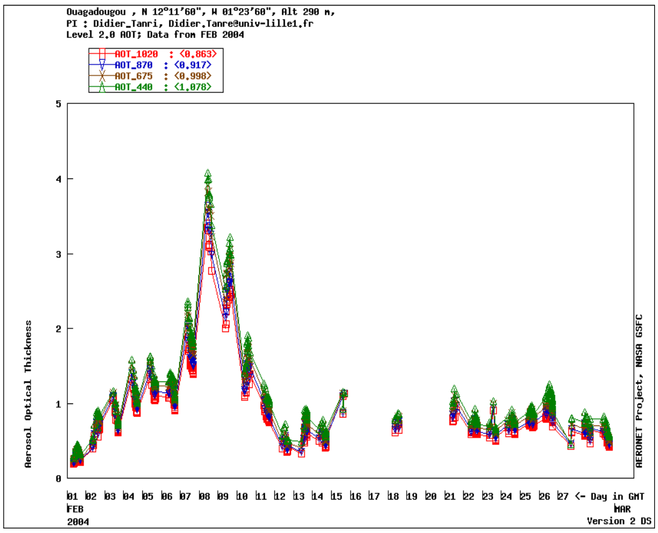

Fig.6(e): Ouagadougou AOT peak of February 09, 2004

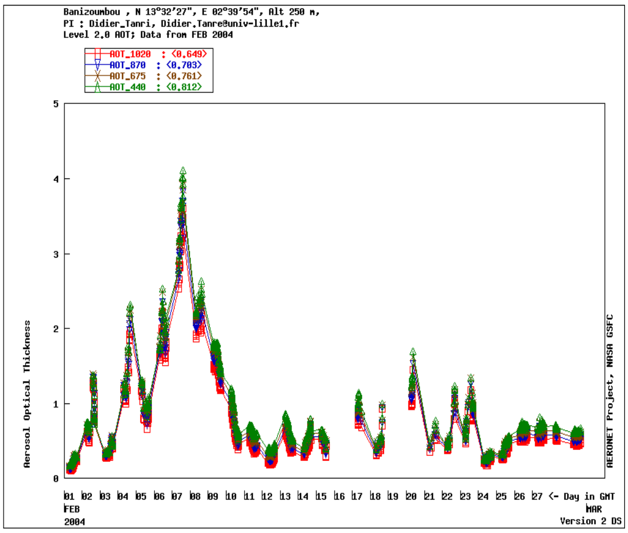

Fig.6(f): Banizoumbou AOT peak of February 08, 2002

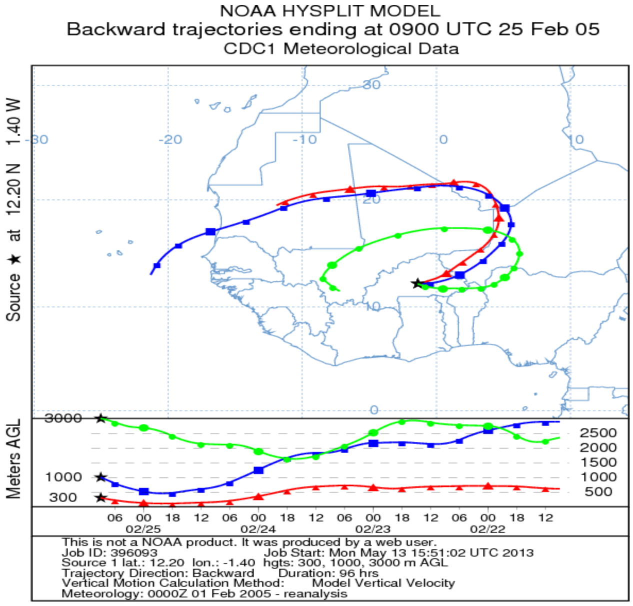

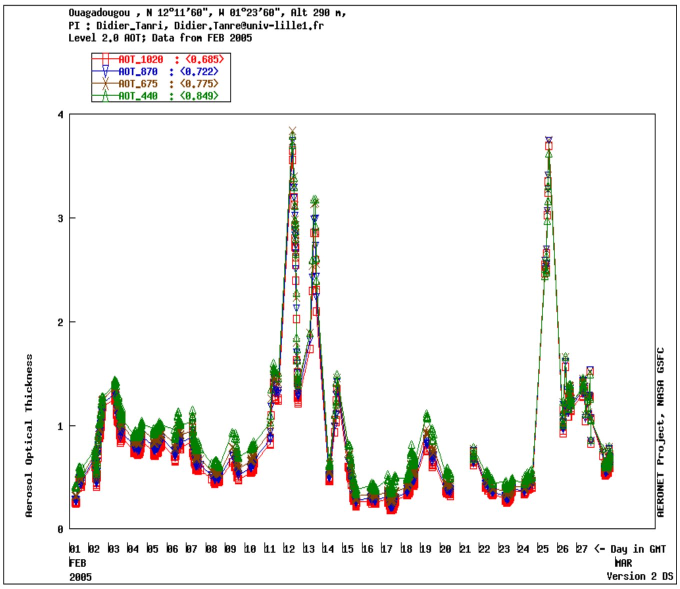

Fig.6(g): Backward trajectories, Ouagadougou Feb 25, 2005 **Fig.6(h)**: Ouagadougou AOT peak of February12 and 25 2005

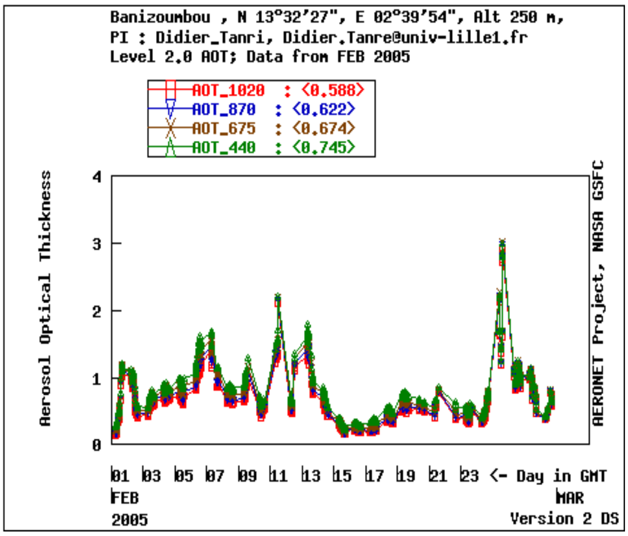

Fig.6(i): Banizoumbou AOT peak of Feb 11 and 25, 2005

The secondary peaks in May and October are usually the effect of uprisings caused by the turbulence associated with the meeting of monsoon and harmattan winds during the rise north of the intertropical convergence zone (ITCZ) at the beginning of the monsoon and its descent south at its end (Bou Karam *et al*, 2008; Marsham *et al*., 2008. Knippertz, 2008). These uprisings are generally not large scale but justified by local winds (Wolfgang Schwanghart and Brigitta Schütt, 2008).

CONCLUSION

The combined analysis of the optical thickness and the trajectories of air masses over Ouagadougou shows a characteristic seasonal variability. According to data collected, the cycle of monsoon winds and harmattan is observed at heights of 300 and 1000m, unlike the 3000m winds that do not follow the same seasonal variability. Climatology of optical thicknesses showed that this quantity is much more in consonance with changes in winds of 300 and 1000m than 3000m, with cyclic peaks between the months of February and March while the lowest values are in the period of monsoon winds (rainy season) and the months of December and January. Our study clearly shows the strong influence of Ouagadougou area Bodélé depression at major airborne dust. This is confirmed by the trajectories and optical thicknesses of Banizoumbou and Ouagadougou. These two places are crossed by the same paths of air at 300m and 1000m and the variabilities of optical thickness present similarities. This gives an indication of the source of emission. We assume that the combined method of trajectories and optical thicknesses can help identify the sources of dust in West Africa and their various zones of influence.

REFERENCES

Baumann, K and Stohl, A., 1997. Validation of a long-range trajectory model using gas balloon tracks from the Gordon Bennett Cup 95. Journal of Applied Meteorology 36, 711-720.

Bou Karam, D., Flamant, C., Knippertz, P., Reitebuch, O., Chong, M., Pelon, J and Dabas, A., 2008. Dust emissions over the sahel associated with the West African monsoon inter-tropical Discontinuity region : A representative case study. Q.J.R. Meteorol. Soc. 134, 621-634

Byers, H. R., 1974. General Meteorology, 4th Edn. McGraw- Hill, New York, U.S.A.

Cabezudo, B., Recio, M., Sanchez-Laulhe, J. M., Trigo, M., Toro, F. J and Polvorinos, F., 1997. Atmospheric trans- portation of marihuana pollen from North Africa to the southwest of Europe. Atmospheric Environment 20, 3323- 3328.

Chiapello, I., Bergametti, G., Chatenet, B., Bousquet, P., Dulac, F and Santos Soares, E., 1997. Origins of African dust transported over the northeastern tropical Atlantic. Journal of Geophysical Research 102, 13, 701-13,709.

D'Abreton, P. C and Tyson, P. D., 1996. Three-dimensional kinematic trajectory modelling of water vapour transport over Southern Africa. Water SA 22, 297-306.

D'Almeida, G. A., 1987. On the variability of desert aerosol radiative characteristics. *J. Geophys. Res* 92(D3), 3017-3026.

Draxler, R., 1998. An overview of the HYSPLIT modeling system for trajectory and dispersion applications,www.arl.noaa.gov/ready/hysplit4.html

Draxler, R. R., 1996a. Boundary layer isentropic and kinematic trajectories during the August 1993 North Atlantic Regional Experiment Intensive. Journal of Geophysical Research 101, 29,255-29,268.

Dubovik, O and King, M. D., 2000. "A flexible inversion algorithm for retrieval of aerosol optical properties from Sun and sky radiance measurements", J. Geophys. Res., 105, 20,673-20,696,

Dubovik, O., Smirnov, A., Holben, B. N., King, M. D., Kaufman, Y. J., Eck, T. F and Slutsker, I., 2000. Accuracy assessment of aerosol optical properties retrieval from AERONET sun and sky radiance measurements, J. Geophys. Res, 105, 9791-9806,

Dubovik, O., Holben, B. N., Lapyonok, T., Sinyuk, A., Mishchenko, M. I., Yang, P and Slutsker, I., 2002a. Non-spherical aerosol retrieval method employing light scattering by spheroids, Geophys. Res. Lett., 10, 10.1029/2001GL014506,

Dubovik, O., Holben, B. N., Eck, T. F., Smirnov, A., Kaufman, Y. J., King, M. D., Tanré, D and Slutsker, I., 2002b. "Variability of absorption and optical properties of key aerosol types observed in worldwide locations", J. Atmos. Sci., 59, 590-608,

Dubovik, O., 2004. "Optimization of Numerical Inversion in Photopolarimetric Remote Sensing", in Photopolarimetry in Remote Sensing (G. Videen, Y. Yatskiv and M. Mishchenko, Eds.), Kluwer Academic Publishers, Dordrecht, Netherlands, 65-106,

Dutton, J. A., 1986. the Ceaseless wind. An Introduction to the theory of Atmospheric Motion. Dover, New York.

Kahl, J. D and Samson, P. J., 1986. Uncertainty in trajectory calculations due to low resolution meteorological data. Journal of Climate and Applied Meteorology 25, 1816—1831.

Kahl, J. D and Samson, P. J., 1988a. Trajectory sensitivity to rawinsonde data resolution. Atmospheric Environment 22, 1291-1299.

Kahl, J. D and Samson, P. J., 1988b. Uncertainty in estimating boundary-layer transport during highly convective conditions. Journal of Applied Meteorology27, 1024-1035.

Kahl, J. D., Harris, J. M., Herbert, G. A and Olson, M. P., 1989a. Intercomparison of long-range trajectory models applied to arctic haze. Proceedings of the 17th NATO/CCMS I¹M on Air Pollution Model and its Applications, pp. 175-185, Plenum Press, New York.

Kahl, J. D. W., 1996. On the prediction of trajectory model error. Atmospheric Environment 30, 2945-2957.

Knippertz, P., 2008. Dust emisions in the West African heat trough the role of the diurnal cycle of extratropical disturbances, *Meteorol. Z. vol 17, N°5, 001-0011*

Laurent, B., 2005. Simulation des émissions d'aérosols désertiques l'échelle continentale : Analyse climatologique des émissions du nord-est de l'Asie et du nord de l'Afrique, *PhD thesis*, *Université Paris 12*

Laurent, B., Heinold, B., Tegen, I., Bouet, C and Cautenet, G., 2008. Surface wind accuracy for modeling mineral dust emissions: Comparing two regional models in Bodélé case study, *Geophys. Res. doi 10.1029/2007JD009484*

Marsham, J. H., Parker, D. J., Grams, C. M., Taylor, C. M and Haywood, J. M., 2008a. Uplift of saharan dust south of the inter-tropical discontinuity. *J. Geophys. Res*.

Martin, D., Mithieux, C and Strauss, B., 1987. On the use of the synoptic vertical wind component in a transport trajectory model. Atmospheric Environment 21, 45-52.

Maryon, R. H and Heasman, C. C., 1988. The accuracy of plume trajectories forecast using the U.K. meteorological office operational forecasting models and their sensitivity to calculation schemes. Atmospheric Environment 22, 259-272.

Merrill, J. T., Bleck, R and Avila, L., 1985. Modeling atmo- spheric transport to the Marshall islands. Journal of Geo- physical Research 90, 12,927-12,936.

Middleton, N. J., Goudie, A. S., 2001. Saharan dust: Sources and trajectories, transactions of the Institute of British Geographers 26, 165-181

Pickering, K. E., Thompson, A. M., McNamara, D. P and Schoeberl, M. R., 1994. An intercomparison of isentropic trajectories over the South Atlantic. Monthly weather Review 122, 864-879.

Pickering, K. E., Thompson, A. M., McNamara, D. P., Schoeberl, M. R., Fuelberg, H. E., Loring Jr., R. O., Watson, M. V., Fakhruzzaman, K and Bachmeier, A. S., 1996. A trajectory intercomparison. Effects of different input analyses. Journal of Geophysical Research 101, 23,903-23,925.

Prospero, J. M., Ginoux, P., Torres, O., Nicholson, S. E and Gill, T. E., 2002. Environnmental characterization of global sources of atmospheric soil dust identified with the Nimbus 7 Total Ozone Monitoring Spectrometer (TOMS) absorbing aerosol product, *Rev. Geophys. 40, 1002, doi 10.1029/2000RG000095*

Sardeshmukh, P. D and Liebmann, B., 1993. An assessment of low-frequency variability in the tropics as indicated by some proxies of tropical convection. Journal of Climate 6, 569-575.

Seibert, P., 1997. Inverse dispersion modelling based on trajectory-derived source-receptor relationships. Proceedings of the 22nd International ¹echnical Meeting on Air Pollution Modelling and its Applications, Clermont-Ferrand.

Sinyuk, A. O., Dubovik, B. N. Holben, T. F. Eck, F-M. Breon, J. Martonchik, R. Kahn, D. J. Diner, E. F. Vermote, J.-C. Roger, T. Lapyonok, and I. Slutsker., 2007. Simultaneous retrieval of aerosol and surface properties from a combination of AERONET and satellite data, *Remote Sensing of Environnment 107, 90-108.*

Stohl, A., 1998. Computation, accuracy and applications of trajectories - A review and bibliography, Atmospheric environnment, vol 35 N°6, 947-966.

Stohl, A., 1996a. On the use of trajectories for establishing source-receptor relationships of air pollutants. Ph.D. The- sis, University of Vienna.

Stohl, A., 1996b. Trajectory statistics : A new method to establish source-receptor relationships of air pollutants and its application to the transport of particulate sulfate in Europe. *Atmospheric Environment 30, 579-587*.

Stohl, A., Wotawa, G., Seibert, P and Kromp-Kolb, H., 1995. Interpolation errors in wind fields as a function of spatial and temporal resolution and their impact on different types of kinematic trajectories. Journal of Applied Meteorology 34, 2149-2165.

Stunder, B. J. B., 1996. An assessment of the quality of forecast trajectories. Journal of Applied Meteorology 35, 1319-1331.

Schutz, L and Sebert, M., 1987. Mineral aerosol and source identification, Journal of aerosol science, vol 18, issue 1, February 1987, 1-10

Swap, R., Garstang, M., Greco, S., Talbot, R and Gac, J. Y., 1992. Sahara dust in the Amazon basin, *Tellus ser.* B 44, 133-149.

Tyson, P. D., Garstang, M and Swap, R., 1996. Large-scale recirculation of air over southern Africa. *Journal of Applied Meteorology 35, 2218-2236.*

Walmsley, J. L and Mailhot, J., 1983. On the numerical accuracy of trajectory models for long-range transport of atmospheric pollutants. *Atmos.-Ocean 21, 14-39.*

Washington, R. W., Todd, M. C., Middleton, N and Goudie, A. S., 2003. Dust storm sources areas determined with the Total Ozone Monitoring Spectrometer and surface observations. Ann. Assoc. Am. Geogr., 93, 297-313

Wolfgang Schwanghart and Brigitta Schütt., 2008. Meteorological causes of harmattan dust in West Africa, Geomorphology 95, 412-428.